

SpUpNIC (Spectrograph Upgrade: Newly Improved Cassegrain) on the South African Astronomical Observatory's 74-inch Telescope

Lisa A. Crause*^a, Dave Carter^a, Alroy Daniels^a, Geoff Evans^a, Piet Fourie^a, David Gilbank^a, Malcolm Hendricks^a, Willie Koorts^a, Deon Lategan^b, Egan Loubser^a, Sharon Mouries^a, James E. O'Connor^a, Darragh E. O'Donoghue^c, Stephen Potter^a, Craig Sass^a, Amanda A. Sickafoose^a, John Stoffels^a, Pieter Swanevelder^a, Keegan Titus^a, Carel van Gend^a, Martin Visser^a, Hannah L. Worters^a

^aSouth African Astronomical Observatory, P.O. Box 9, Observatory 7935, Cape Town, South Africa

^bDenel SpaceTeq, Electron House, 15 Electron Street, Techno Park, Stellenbosch 7600, South Africa

^cSALT Foundation, P.O. Box 9, Observatory 7935, Cape Town, South Africa

ABSTRACT

SpUpNIC (Spectrograph Upgrade: Newly Improved Cassegrain) is the extensively upgraded Cassegrain Spectrograph on the South African Astronomical Observatory's 74-inch (1.9-m) telescope. The inverse-Cassegrain collimator mirrors and woefully inefficient Maksutov-Cassegrain camera optics have been replaced, along with the CCD and SDSU controller. All moving mechanisms are now governed by a programmable logic controller, allowing remote configuration of the instrument via an intuitive new graphical user interface. The new collimator produces a larger beam to match the optically faster Folded-Schmidt camera design and nine surface-relief diffraction gratings offer various wavelength ranges and resolutions across the optical domain. The new camera optics (a fused silica Schmidt plate, a slotted fold flat and a spherically figured primary mirror, both Zerodur, and a fused silica field-flattener lens forming the cryostat window) reduce the camera's central obscuration to increase the instrument throughput. The physically larger and more sensitive CCD extends the available wavelength range; weak arc lines are now detectable down to 325 nm and the red end extends beyond one micron. A rear-of-slit viewing camera has streamlined the observing process by enabling accurate target placement on the slit and facilitating telescope focus optimisation. An interactive quick-look data reduction tool further enhances the user-friendliness of SpUpNIC.

Keywords: SpUpNIC, Spectrograph, Cassegrain, Optical, Alignment, Instrumentation, SAAO, Upgrade

1. INTRODUCTION

1.1 Instrument History

For four decades, the 74-inch (1.9-m) telescope¹ at the South African Astronomical Observatory (SAAO) field station near the Karoo town of Sutherland has hosted a low resolution spectrograph at its Cassegrain focus. This workhorse instrument has undergone various incremental upgrades over time as critical technologies, particularly astronomical detectors, have evolved. The earliest version of the spectrograph employed an image intensifier that fed a photographic plate. This was later replaced by a photon-counting system, which was followed by a pair of linear photodiode arrays known as the Reticon Photon Counting System (RPCS). The Reticon was superseded in the mid 1990's when a 1798 × 266 Charge Coupled Device (CCD) was introduced and this system remained in use until late 2014.

1.2 The Spectrograph Upgrade² Project (SpUp)

In October 2014, the old spectrograph (aka Cassie) was taken out of service for a year to allow the instrument team to perform a long-awaited upgrade. The original plan, in the late 1990's, had been to replace the spectrograph's camera optics to increase the throughput of the system. These new optics were designed and manufactured, before being packed in a closet for safe keeping while the focus of the SAAO shifted to the construction, instrument development, commissioning, troubleshooting and running of the Southern African Large Telescope (SALT)³⁻¹¹.

* lisa@sao.ac.za

Over the intervening years, the Cassegrain Spectrograph Upgrade received intermittent background attention and thus the project was subject to an unprecedented level of scope creep. The eventual upgrade centred on replacing the entire lower box of the spectrograph – the section containing the collimator and camera optics, the detector system and various electro-mechanical mechanisms. The upper box (that houses the acquisition and guidance hardware and optics, the filter wheel and the slit mechanism) did not change substantially, but all of those components were cleaned and/or repaired to improve their performance and reliability. A programmable logic controller (PLC) was introduced to place all of the moving mechanisms (pneumatic actuators and stepper motors) and on/off toggles for lamps within the instrument under software control. This rendered almost every aspect of the spectrograph remotely configurable, which in turn has allowed automation of routine processes through the new instrument control software. This Python-based graphical user interface for SpUpNIC is supported by the SAAO’s new instrumentation software framework (described elsewhere in these proceedings by van Gend et al.), as is the associated quick-look data reduction tool that was introduced to automatically extract and wavelength calibrate the spectra.

Consequently, the latest incarnation of the spectrograph is effectively a brand new instrument, with every sub-system having been extensively improved or completely replaced. The resulting increase in scientific capability breathes new life into our treasured 74-inch telescope and the SAAO Instrumentation group has gained invaluable practical expertise that will be incorporated into future instrument development projects. In particular, the SAAO Mechanical Workshop was deliberately challenged by an assortment of complex mechanical designs that demanded expert use of the Observatory’s superb array of computer numerical control (CNC) machines, including a wire-cutter, a spark-eroder, a large CNC lathe and a 5-axis CNC mill.

2. INSTRUMENT DESCRIPTION

2.1 Basic Layout

When in use, SpUpNIC bolts to the Cassegrain weight plate, which is attached to the instrument rotator flange located behind the primary mirror. While other instruments are in operation, the spectrograph is secured to a trolley and stored in a room adjacent to the observing floor. Both this trolley and the frame used to attach the spectrograph to the telescope were modified to accommodate the changes associated with the upgrade (see Fig. 1).



Figure 1. The old Cassegrain Spectrograph (aka Cassie) on the 74-inch telescope (left) and the upgraded instrument (SpUpNIC) shortly after installation in October 2015 (right).

Figure 2 shows SpUpNIC on its instrument trolley prior to installation on the telescope, and Figure 3 provides a detailed breakdown of the system in the form of a block diagram. Here we start with an overview of the system, broadly

distinguishing the functionally different upper and lower parts of the spectrograph, before delving into the specifics of the individual sub-systems in subsequent sections.

The top portion of the instrument, referred to as the *upper box*, is largely concerned with the acquisition and wavelength calibration processes. All of the associated components were worked on and improved, but none were replaced. Given the history of the instrument, it seems appropriate that the original slit mechanism (where the spectrograph technically begins) has been retained.

The *lower box* houses the spectrograph optics (the collimator, diffraction grating and camera) and the detector. It is the replacement of the collimator and camera optics that has significantly increased the throughput of the instrument. An additional USB camera with associated relay optics was also introduced to the lower box to streamline the acquisition process, particularly for the fainter targets rendered observable by the improved throughput of the spectrograph.

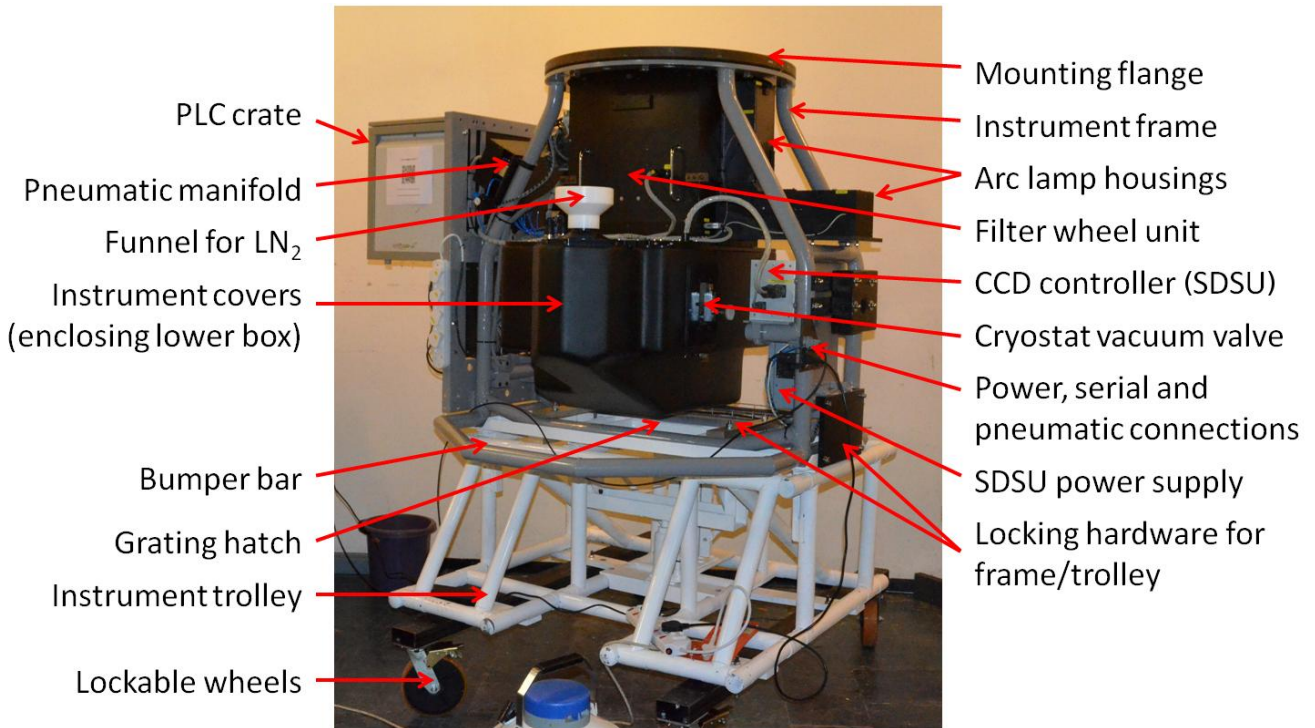


Figure 2. This shows the external layout of SpUpNIC, corresponding to a view from the north-west side of the dome when the instrument is mounted on the telescope.

2.2 Upper Box: Acquisition and Calibration Hardware

Acquisition Mirror

The upper box contains a large 45° flat mirror with a central hole. This is the acquisition/guide mirror, which needs to be horizontally offset for acquisition and centred during an observation to allow light to reach the spectrograph slit. An external XY slide unit carrying the main acquisition camera attaches to the south side of the upper box. The slides can move the acquisition camera anywhere around the annular field of view for offset guiding during an exposure. This dusty mirror with its hugely degraded coating was removed, stripped with ferric chloride, washed with a soap solution, and thoroughly rinsed with de-ionised water before being re-aluminised and re-installed – see (1) in Fig. 4. The relay optics for viewing the slit (from above) with the acquisition camera were also cleaned and re-installed.

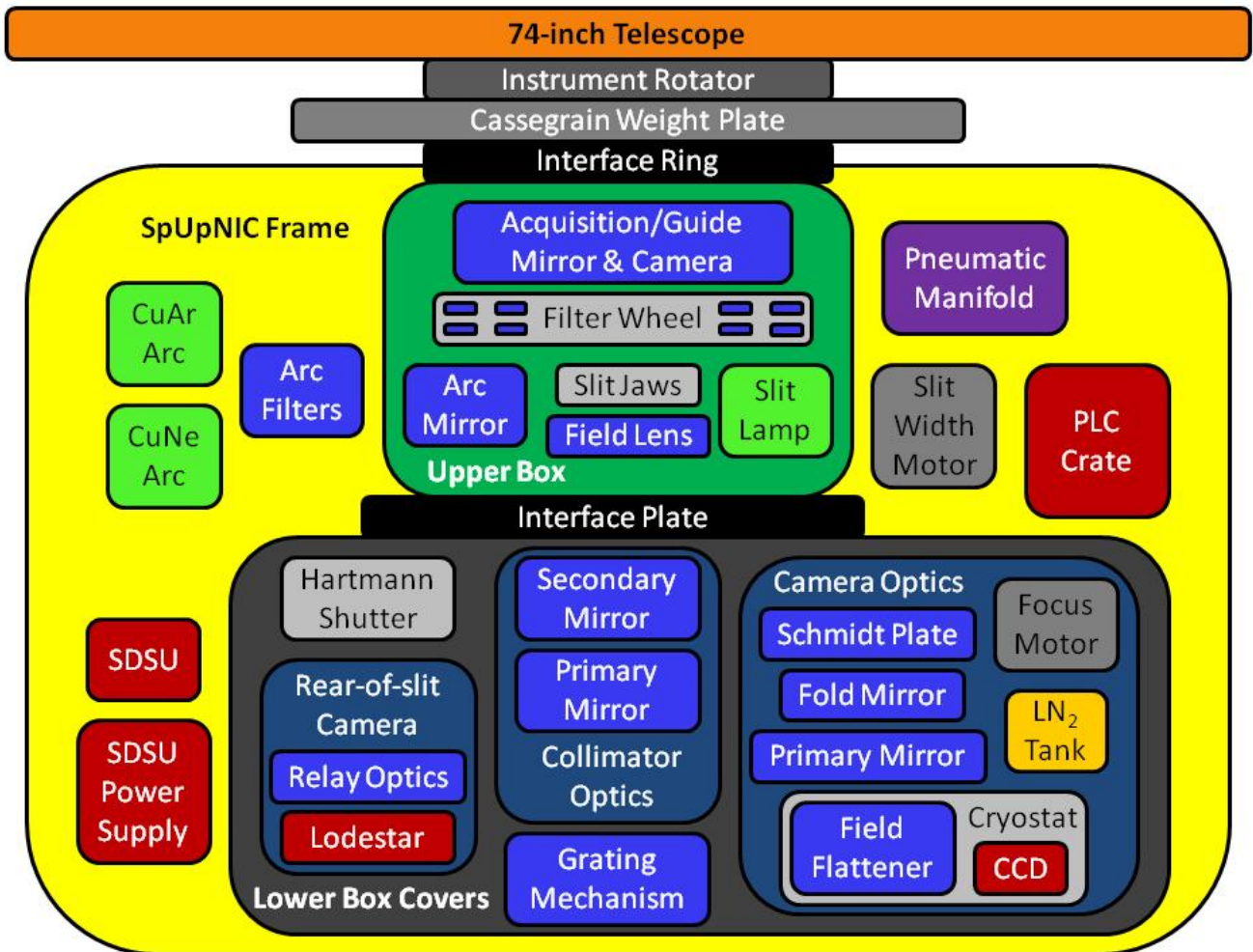


Figure 3. Block diagram for SpUpNIC. Orange represents the telescope, yellow the instrument frame, dark green the upper box, black the lower box, optical elements/assemblies are blue, electronics are red, lamps are light green, mechanical components are various shades of grey, the manifold for the pneumatic system is purple and the liquid nitrogen tank for cooling the CCD is shown in yellow/orange.

Filter Wheel

The spectrograph has a filter wheel, see (2) in Fig. 4, containing a set of neutral density filters for bright objects, one open slot and various order blocking filters (BG38, BG39 and GG495) that are to be used with certain gratings. The ancient filter set was severely degraded so they were replaced and new filter holders were designed and manufactured. Removing the filter wheel unit opens up the north side of the upper box and provides access to the slit mechanism.

Arc Lamps

SpUpNIC has two hollow-cathode arc lamps (CuAr and CuNe) for wavelength calibration. Previously, users had to manually swap the lamps depending on the grating being used. One of the lamp housings was modified to allow light from either (or both) of the lamps to be injected with a software toggle, rather than requiring a mechanical intervention. The individual arc filters for the lamps still need to be manually inserted and removed for certain gratings, but that is a relatively trivial task that would have been problematic to automate. The arc filter requirements for the different gratings are listed in Table 1.

Slit Mechanism

Astronomical targets are positioned on the entrance slit of the spectrograph, the full length of which corresponds to 2 arcminutes on the sky. The width of the slit may be adjusted from 25 to 700 microns in 25 micron increments (0.15 to 4.2 arcseconds in 0.15 arcsecond increments) to suit the atmospheric seeing conditions and the resolution requirements of the user. The slit assembly from the original Cassegrain spectrograph was given an extensive overhaul. The slit shutter mechanism was removed, the slit jaws were cleaned and the retaining springs were replaced, as was the pneumatic cylinder for actuating the small 45° mirror that deploys to direct arc light into the spectrograph for calibration frames. The mounting assembly for the gearbox that controls the slit width was replaced to eliminate misalignments that stressed the motor coupling and the plano-convex field lens, see (3) in Fig. 4, located beneath the slit was replaced to match the new collimator optics. The LED used to illuminate the slit was retained.

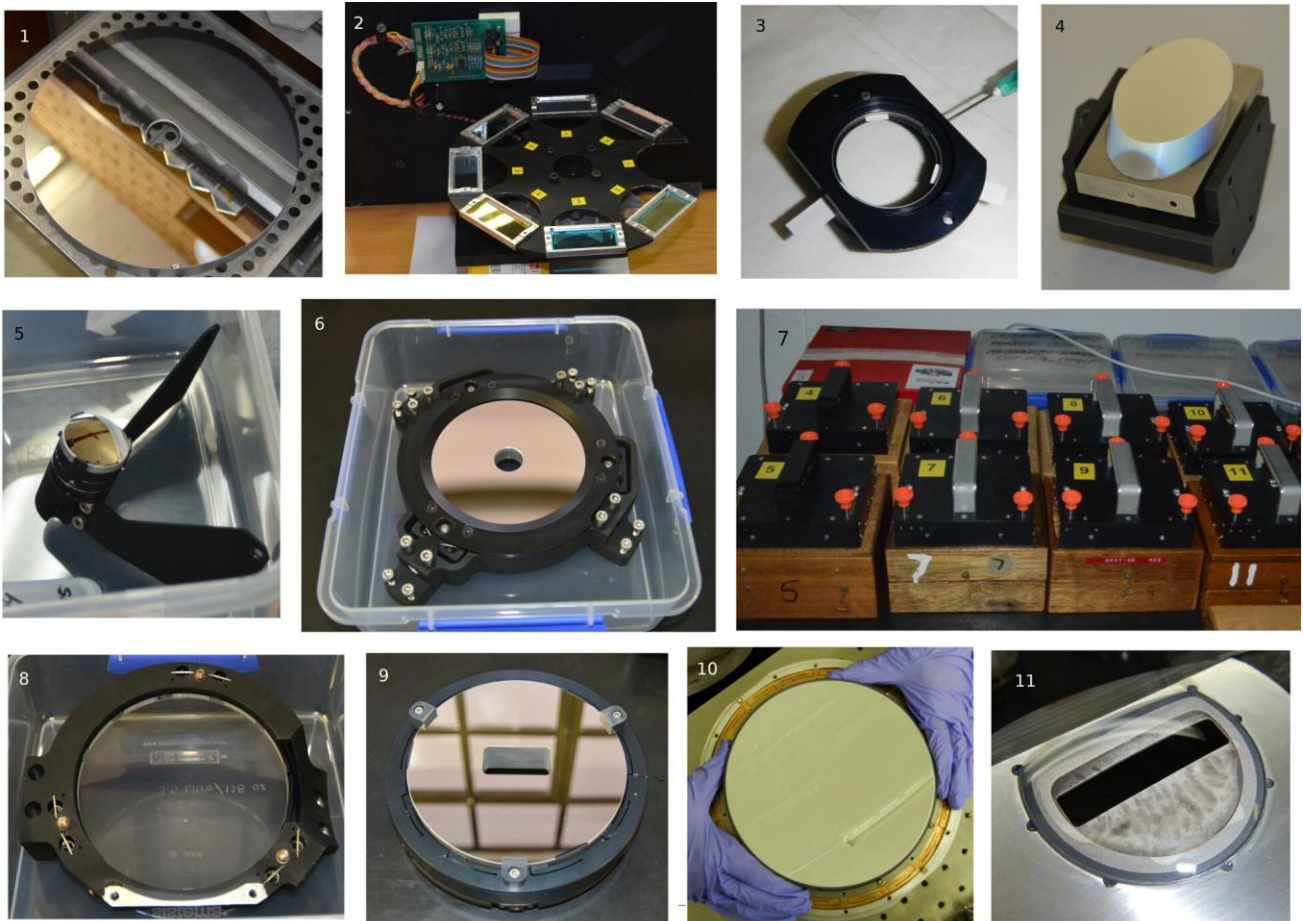


Figure 4. All of the SpUpNIC optical elements: 1 = flat acquisition/guide mirror, 2 = filter wheel, 3 = plano-convex field lens, 4 = rear-of-slit fold mirror, 5 = hyperbolic collimator secondary mirror, 6 = parabolic collimator primary mirror, 7 = surface-relief diffraction gratings, 8 = Schmidt plate, 9 = slotted camera fold mirror, 10 = spherical camera primary mirror, 11 = biconvex field-flattener lens forming the cryostat window.

2.3 New Lower Box: Spectrograph Essentials

Instrument Covers

A two-part carbon fibre cover forms a light- and dust-tight enclosure protecting the delicate contents of the lower box. A hatch on the underside of the south cover provides access to the grating mechanism, the vacuum valve of the cryostat protrudes through a port on the west side of the north cover and test points for the CCD pre-amp are accessible through a small port on the top of the interface plate.

Hartmann Shutter

The spectrograph needs to be focused whenever a different grating is inserted, and since the focus varies with temperature, it should be checked daily (and during the night if the temperature changes substantially). The two semi-circular Hartmann shutters used to focus the old spectrograph were replaced with a single shutter that is driven by a pair of pneumatic cylinders. Actuating one cylinder causes the shutter to block one half of the beam (between the two collimator mirrors) and then the second cylinder moves the shutter so as to block the other half. Retracting both cylinders stows the shutter out of the beam. With all the SpUpNIC mechanisms under software control via the new programmable logic controller (PLC), the previously cumbersome focusing process has been automated.

Rear-of-slit Camera

A new optical system was added to the instrument to view the slit from below. This offers a more reliable way to ensure proper target placement on the slit prior to auto-guiding and taking spectra, and it is painless to periodically check the target position during multiple exposures. A small fold mirror, see (4) in Fig. 4, is pneumatically inserted into the beam between the two collimator mirrors. The mirror directs light from the spectrograph slit, via an achromatic doublet lens, to a compact USB-powered Starlight Xpress Lodestar camera that projects through the front of the south cover. This camera is permanently focused on the slit, so if an object appears out of focus, one simply needs to adjust the telescope focus. The camera is sensitive enough that exposures of a couple of seconds suffice for targets with $V \sim 18$ mag.

Collimator Optics

SpUpNIC's predecessor employed an F/2.2 inverse-Cassegrain collimator (a backwards telescope), but the instrument had previously also used an F/1.4 collimator unit. The optically faster new camera design would benefit from the larger beam of the F/1.4 collimator, so after tracking down that set of mirrors and establishing their optical properties, we elected to also replace the entire collimator unit (and, hence, the field lens below the slit). Since all of the collimator and camera optics were to be bonded into their cells, we would not be able to recoat them periodically. Thus we opted for the slightly lower reflectivity, but greater durability, of protected-aluminium coatings on the various mirrors. The collimator's hyperbolic secondary and parabolic primary mirrors are shown in (5) and (6), respectively, in Fig. 4.

Diffraction Gratings

The nine surface-relief diffraction gratings from the old spectrograph were retained – their properties are listed in Table 1. New grating housings, see (7) in Fig. 4, were magnetically encoded to allow grating information to be automatically incorporated into the file headers. The required grating still needs to be manually bolted into the frame of the grating mechanism, via a hatch on the bottom of the south cover. Setting the desired wavelength range is much simpler though as the grating angle has been motorised. Thus the process no longer requires iterative mechanical adjustments to be made to the grating angle from up the ladder, and the software also provides automatic wavelength identification.

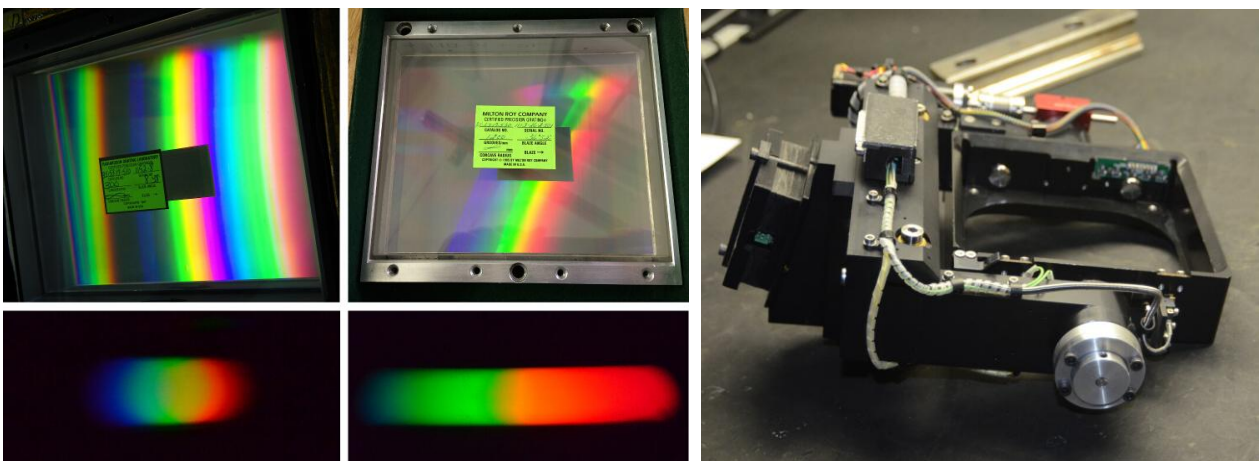


Figure 5. SpUpNIC's lowest dispersion (300 lines/mm) diffraction grating, along with its resulting spectrum below, is shown on the left. The highest dispersion (1200 lines/mm) grating is shown in the centre. The grating mechanism sub-assembly (right) holds individual grating cells and since it is motorised, users can set the desired wavelength range (by adjusting the grating angle) via the instrument control GUI.

Camera Optics

The old Maksutov-Cassegrain camera's large central obscuration made the spectrograph extremely inefficient. So late last century, a new Folded-Schmidt camera was designed and custom optics were manufactured. These elements (see Fig. 4) are: a fused silica Schmidt plate (8), a Zerodur fold mirror with a central slot (9), a spherical primary mirror also made of Zerodur (10) and a sawn-off fused silica field-flattener lens (11) that doubles as the cryostat window. An anti-reflection coating (likely MgF_2) had been applied to the refractive optics, but the mirrors had yet to be coated. We again chose a robust protected-aluminium coating to permit cleaning of the camera mirrors. The fold mirror has a recess cut in the back to allow the cryostat unit to nestle into that space, so that the cryostat window/field-flattener lens can locate immediately behind the slot in the mirror and place the CCD at the focal plane.

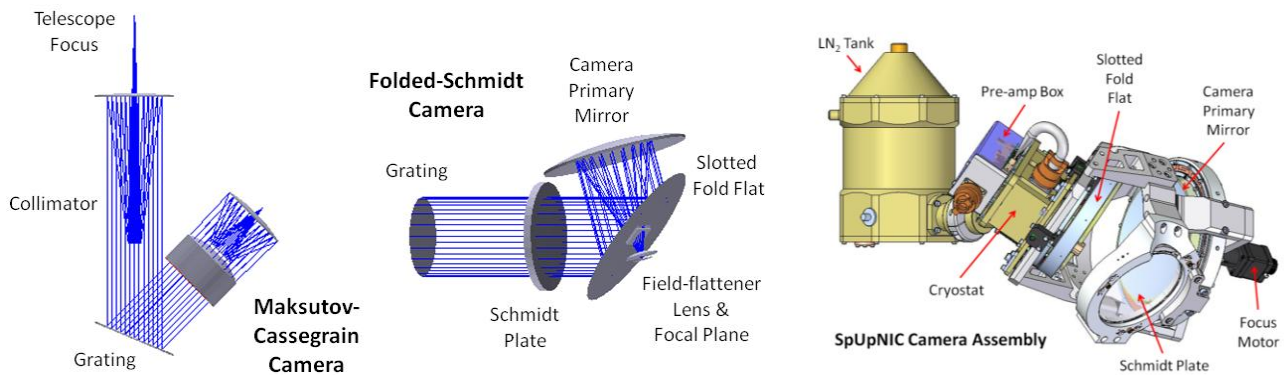


Figure 6. Zemax ray tracings for the old Maksutov-Cassegrain camera (left) and the new Folded-Schmidt camera (centre). The CAD model (right) shows the new camera assembly, including the cryostat and the liquid nitrogen tank for cooling the CCD.

The SpUpNIC camera employs an elegant focus mechanism that yields pure, high resolution axial translation of the camera primary mirror over a large (3 mm) range. The mirror is mounted within a radial flexure ring and supported from below on three hard points (formed by tip/tilt fine-adjusters contacting invar pads bonded to the back of the mirror) in the base-plate. The outside of the radial flexure ring is connected above and below to a pair of 250 micron thick, wire-cut beryllium-copper flexure rings, which in turn connect to an outer ring that is fixed to the supporting frame holding the stepper motor. The motor is connected to the base plate and thus drives the mirror back and forth, with the flexures providing radial stiffness and axial compliance. Careful alignment of the motor axis (via the three tip/tilt screws) to less than an arcminute over the full range of travel (only a tenth of which is required to focus the spectrograph) was achieved with the aid of the finely graduated reticule of a TriOptics auto-collimator.

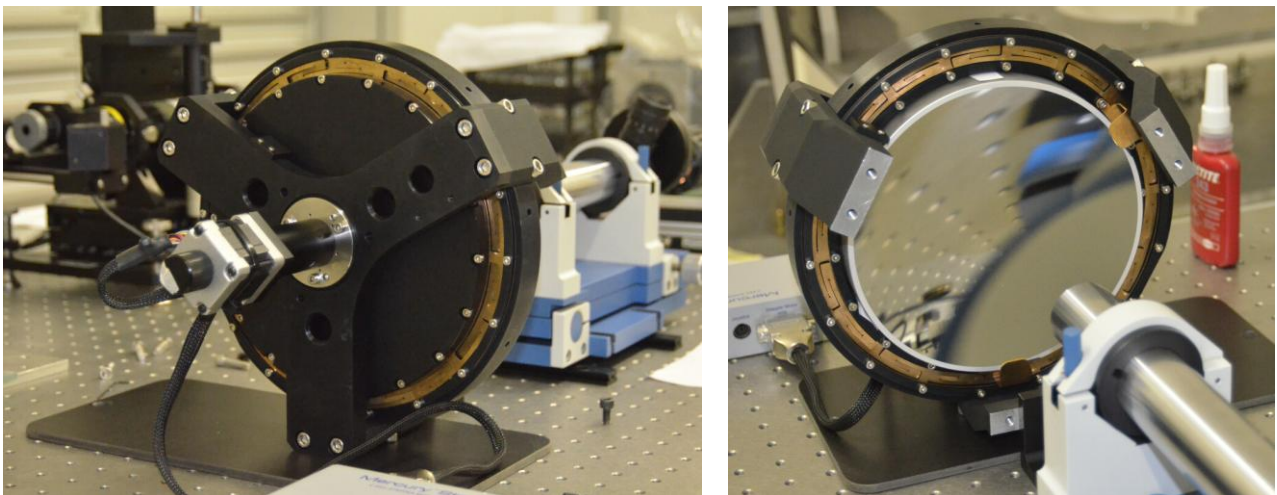


Figure 7. The SpUpNIC focus mechanism, consisting of a stepper motor that drives the camera primary mirror back and forth with radial constraint provided by a pair of 250 micron thick wire-cut beryllium-copper flexures.

Cryostat

The complexity of the SpUpNIC cryostat is best appreciated by viewing the cryostat assembly video, filmed in the SAAO CCD lab during the process. The clip is too long to include in this manuscript, but it is available at www.youtube.com/watch?v=XAkJJY5ZPZO. The final optical element of the camera is bonded (with Scotch-Weld 2216 epoxy adhesive) to the aluminium cryostat housing. Since this biconvex lens forms the cryostat window, it needs to hold vacuum so the system was multiply leak tested with a residual gas analyser (aka “helium sniffer”). A small leak developed after the first rigorous clean of the cryostat, but this was successfully repaired with additional epoxy. The copper block that provides thermal contact between the cold finger (which is connected to the base of the liquid nitrogen tank) and the back of the CCD also carries a small resistor to prevent the CCD from getting too cold. Extensive thermal testing was done to tune the lengths and thicknesses of the copper braids inside the cryostat to establish the optimal CCD operating temperature. A single-piece titanium cradle supports the chip and a kinematic, stainless steel alignment jig was designed to allow precise axial positioning and optical alignment of the CCD to the field-flattener lens before the cradle was bonded. This process was particularly delicate as any focal plane misalignments could severely compromise the image quality of the spectrograph. The alignment and bonding of the CCD cradle is described in Section 3.2.

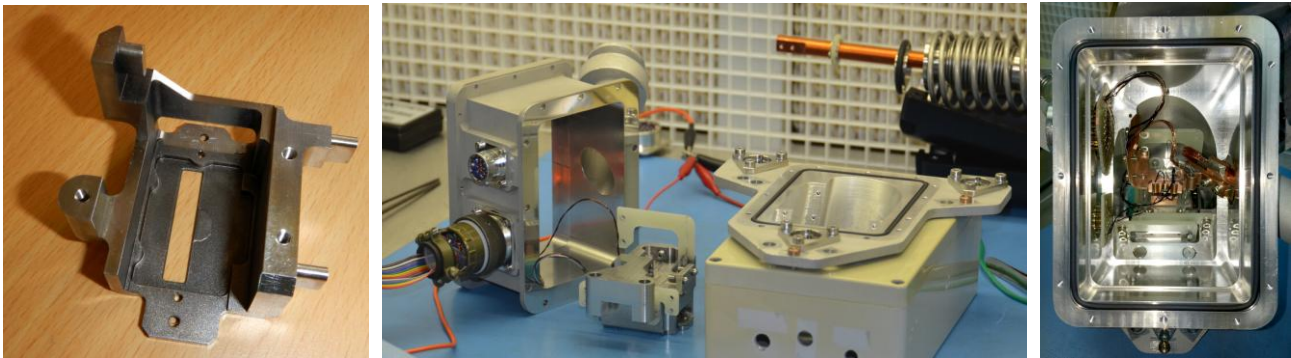


Figure 8. The single-part titanium cradle that carries the CCD is shown on the left. The central photo shows the various cryostat components (the upper section with its hermetic connectors, the CCD cradle with its kinematic alignment jig attached, and the lower section that includes the cryostat window and which carries the CCD). The complete assembly, seen from above before attaching the lid, is shown in the photo on the right.

Detector System

The new SpUpNIC detector is an E2V CCD42-10 CCD with 2048×512 pixels, each 13.5 microns on a side. Although the detector is not configured for frame transfer readout, one half of the chip is masked off and pseudo frame transfer readout is implemented. Consequently, only half of the vertical extent of the $27.6 \text{ mm} \times 6.9 \text{ mm}$ imaging area is used, corresponding to the slit spatially sampling 120 arcsec on the sky. A broad-band anti-reflection coating was applied to the CCD, which is thinned and back-illuminated so that its quantum efficiency peaks in the green. The data sheet quotes QE values of 50% at 350 nm, 85% at 500 nm, 70% at 650 nm and 35% at 900 nm. The chip has an extremely low noise amplifier and the CCD is usually 1×2 binned (in the spatial direction) to increase the signal-to-noise ratio. Thermal/electronic noise is minimised by cooling the CCD to $-105 \text{ }^\circ\text{C}$ with liquid nitrogen. The system has four modes offering different gain/readout-speed combinations: Faint/Slow, Faint/Fast, Bright/Slow and Bright/Fast. Faint/Slow mode, with its gain of 1.145 electrons/ADU and read-noise of 2.57 electrons RMS is the most commonly used, as it allows faint targets to utilise the full dynamic range of the analogue-to-digital converter. The Bright/Fast setting (5.54 electrons/ADU gain and 6.68 electrons RMS read-noise) is more suitable for bright targets that will require most of the pixels' full well depth to avoid saturation. SpUpNIC is the first SAAO instrument to employ the SDSU Generation III CCD controller architecture, a transition that presented its share of challenges.

2.4 Software

The instrument software follows a distributed architecture, with drivers for individual hardware components (the PLC and the detector system) implemented as stand-alone server processes. These are connected to corresponding clients

over TCP/IP sockets. The clients are bundled together and instantiated by a controller class, on top of which is a user interface implemented in Python using the Qt widget set. The Instrument Control software graphical user interface (GUI) includes an interactive schematic representation of the instrument that may be used to configure the system, either for acquisition, calibration or target observations. This simple, intuitive interface makes it easy to toggle lamps and mirrors, and to see if the system is not set up for a science exposure, since a blue frame appears around the graphic if anything is out of place. Previously it was not uncommon to accidentally take a long science exposure without realising that a mirror had been left in the beam, or a calibration lamp had been left on. The new software thus streamlines the observing process and reduces the amount of time that might be wasted by such mistakes during viable observing time. SpUpNIC also has a new quick-look data reduction GUI that displays extracted, sky-subtracted, wavelength-calibrated spectra as soon as the data are saved at the end of an exposure. Extraction and sky subtraction regions, smoothing and display options can be changed on the fly and the output is automatically saved as a simple text file suitable for plotting, or these .txt files can easily be converted into a .fits file (e.g. using the *rspectext* task in *IRAF*).

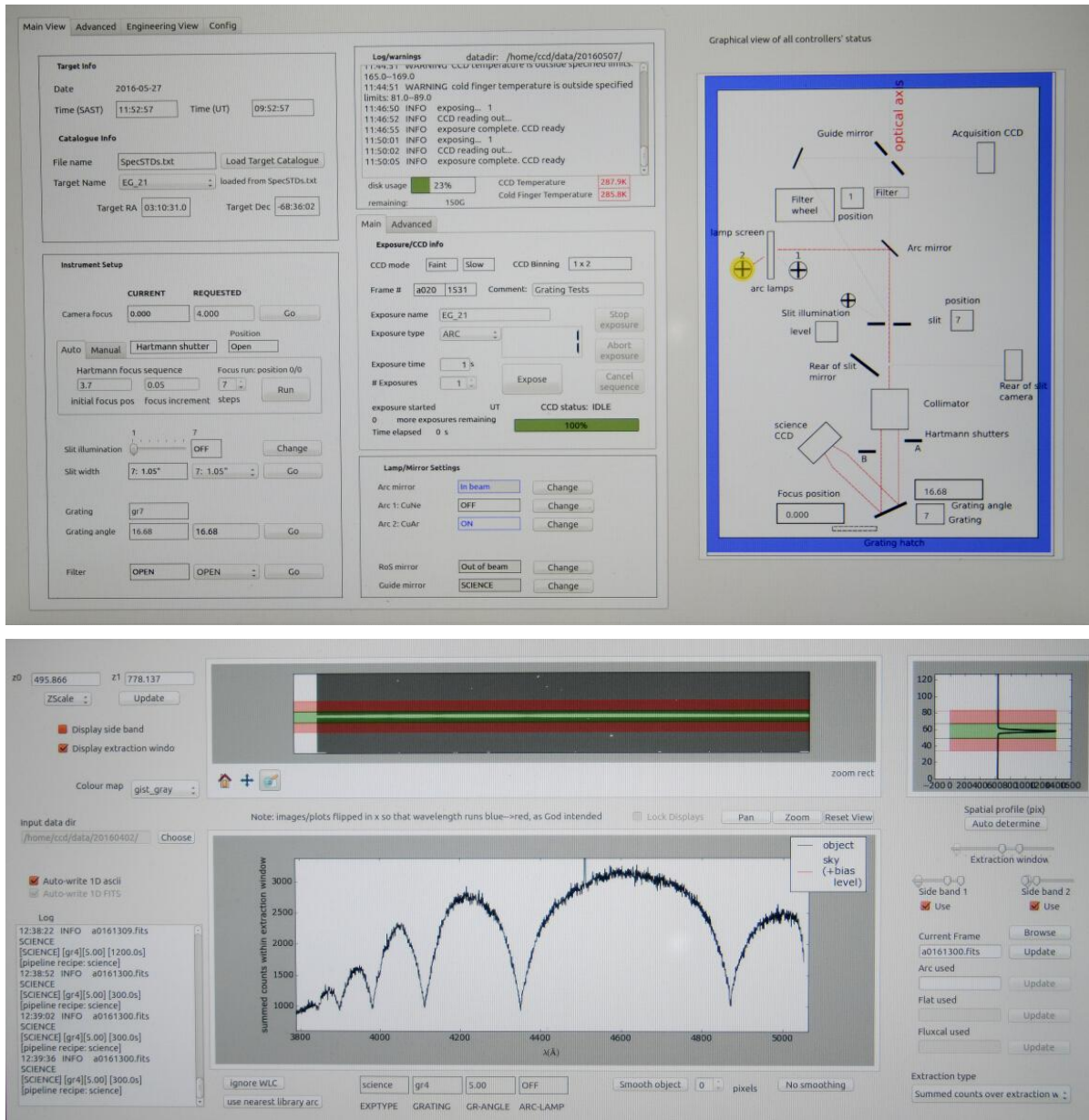


Figure 9. SpUpNIC graphical user interfaces for the instrument control software (top) and quick-look data reduction tool (bottom).

3. INTEGRATION, ALIGNMENT AND BONDING OF THE OPTICS

3.1 Optical Integration

All of the new SpUpNIC optics were bonded into their housings with Scotch-Weld 2216 epoxy before being integrated into their cells. The field lens and field-flattener lens did not require special alignment so no adjustability was provided. Since the camera primary mirror was defined to be the reference optic and as it provides focus compensation for the spectrograph, it only required tip/tilt adjustability. The cells for all of the other elements were fully adjustable in tip/tilt, decentre and focus, using combinations of 100 TPI fine adjustment screws, wire-cut flexures and spring plungers. The collimator mirrors, Schmidt plate and camera fold mirror were bonded into their respective radial flexures before being integrated into their opto-mechanical cells. The collimator and camera mounting assemblies are shown in Figures 10-12.



Figure 10. The collimator secondary mirror and wire-cut flexure mounts for decentre adjustment (left) and the complete assembly that includes tip/tilt and focus adjustability (right).



Figure 11. The collimator primary mirror bonded into its radial flexure (left) and the mirror cell with its pairs of decentre adjusters and the three tip/tilt adjusters that also provide focus travel (centre). The assembly is held together by three pairs of spring hooks with dowels locking each end. The grey patches of epoxy are visible through the back of the mirror (right).

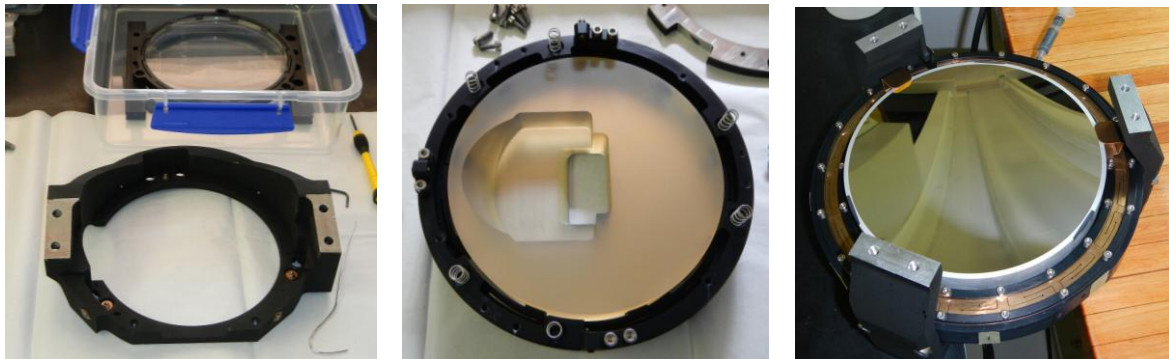


Figure 12. The Schmidt plate (left), and fold mirror (centre) were bonded into their radial flexures before integration into their cells. The camera primary mirror had to be aligned in tip/tilt to place the spectrum on the CCD (right) before it could be bonded.

3.2 Optical Alignment

Close attention was paid to the interface between the old and new sections of the instrument, and concerns regarding the preservation of the optical axis of the old spectrograph gave rise to a 74-inch alignment project – described in these proceedings by Booth et al. A procedure was developed to align the telescope mirrors, so that the optical axis of the 74-inch emerges through the centre of, and perpendicular to, the instrument mounting flange. This telescope alignment process will be performed whenever the mirrors are re-installed after aluminising, or if the system is otherwise disrupted.

Having carried out this process, the upper and lower boxes of the spectrograph could be optically aligned with respect to the mounting interface, so that bolting the instrument to the telescope would reliably place SpUpNIC on the optical axis of the 74-inch. This was done using a Taylor-Hobson micro-alignment telescope (AT), modified to include an LED (with brightness control) and a tiny (<10 micron) pinhole on an arm that projects across the front of the AT. This arm is on an adjustable flexure, allowing the LED to be exactly aligned to the AT crosshairs and locked in position. As a result, every optical surface illuminated by the AT produces a bright reflection, which can be used to align the optic by centring the return spot in the AT. The spots from each optical surface may be viewed in turn by adjusting the focus knob of the AT*.

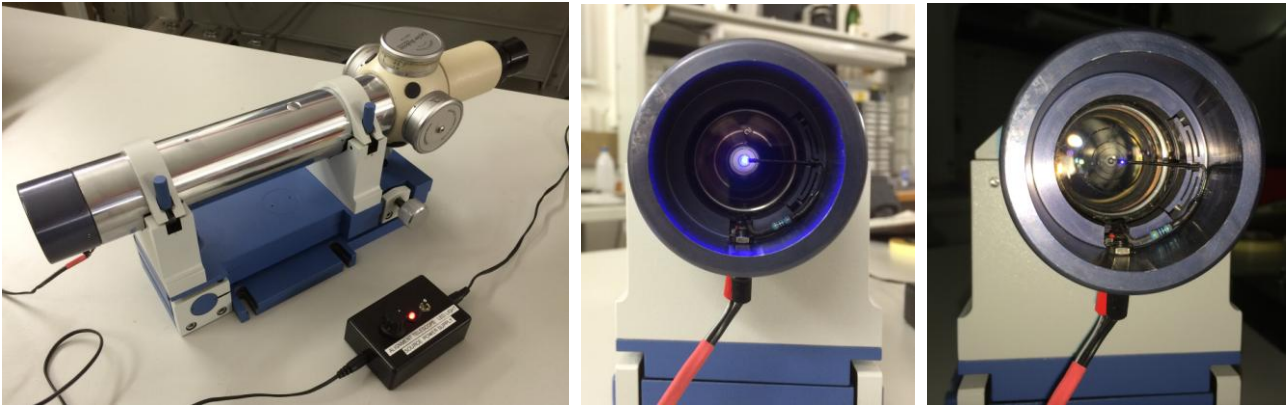


Figure 13. Extremely useful modifications were made to an alignment telescope (AT) to introduce an adjustable brightness LED on an arm that extends to the centre of the field. Every optical surface illuminated with the AT then produces a bright reflection, each of which can be viewed by adjusting the focus knob of the AT.

The AT was centred on a set of crosswires (carefully strung across the mounting flange on the top of the upper box), and squared up to a rear-surface mirror in contact with the flange. The return spots from the two surfaces of the field lens (located behind the open slit) could be viewed with the AT and used to adjust the slit unit to align it to the centre of the instrument mounting interface.

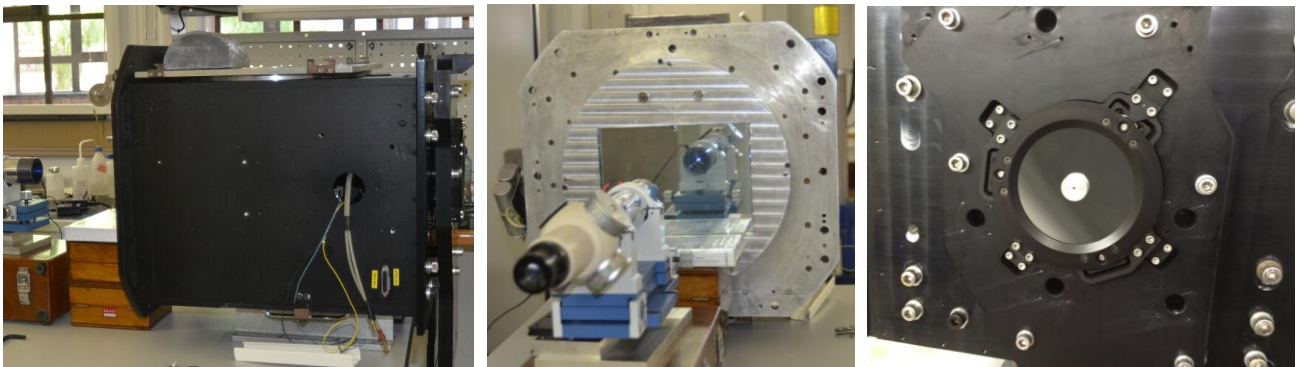


Figure 14. The upper box lying on its side (left) so that the alignment telescope (centre) could be used to align the slit unit and the collimator primary mirror (mounted within the top plate of the lower box, which was bolted to the interface plate), right.

* This invaluable addition to an already priceless optical alignment tool is thanks to the genius of Francois Strümper, who previously brought us the brilliant hands-free Faro Arm trigger¹²!

The aligned slit unit was drilled and pinned to capture its position on the interface plate between the upper and lower boxes. The top plate of the lower box (housing the collimator primary mirror) was then attached to the upper box and the collimator primary was aligned (in tip/tilt and decentre) to the optical axis (see Fig. 14). Two aluminium plugs, one with a small central hole and another with a central cross, were made to locate in the hole in the collimator primary to provide a target for the AT. The top plate of the lower box could then also be drilled and pinned to preserve its position with respect to the upper box. Both the top plate and the slit unit could then be removed and used to align the lower box.

A custom jig was designed and built to allow the entire lower box structure to be rotated and firmly locked at any angle about a horizontal axis. An assortment of alignment gear could then be set up on an optical bench in the lab and directed into the instrument during various stages in the alignment process (see Figs 15 and 16).



Figure 15. Bolting the instrument to the alignment jig (left) required everything to be upside down, but the alignment process was done with the jig rotated through 90° and then securely locked in that position (right).

A Buccini MIC-1 laser interferometer was used to align the SpUpNIC collimator unit in double-pass, with an old diffraction grating operating in zeroth order serving as the flat mirror. A variable beam expander and a focusing lens were used to convert the collimated interferometer output to an F/18 input beam, to match what the 74-inch delivers at its Cassegrain focus. The collimator alignment mostly involved tip/tilt and decentre adjustment of the secondary mirror (since the primary mirror was aligned and locked when working with the upper box), but the process also included some adjustment of the grating mechanism. Early efforts required translation of the slit unit as well to centre up the field lens, but this was eliminated later, once the slit mechanism had been pinned in the required position.

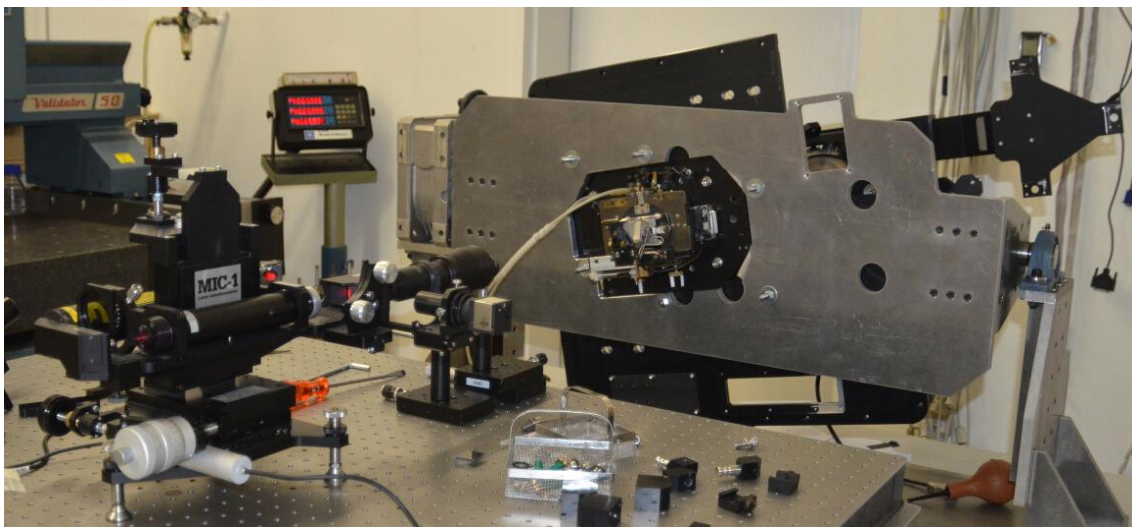


Figure 16. The optical alignment setup for SpUpNIC included a MIC-1 interferometer and various optics used to produce an F/18 beam that could be focused on the slit assembly.

Aligning the camera optics was a matter of trial and error, with occasional reference to the Zemax model, particularly the footprint diagrams for each optical surface. The Schmidt plate is relatively insensitive to misalignment due to its low optical power, but correctly positioning the slotted fold mirror and the camera primary mirror was more important. The slot in the fold mirror had to hide as much of the central obscuration (from the collimator secondary mirror, which in turn hides the equivalent obscuration from the telescope) as possible. Then the camera primary mirror was adjusted in tip/tilt to steer the converging beam through the slot without vignetting en route to the detector. The cryostat unit, housing the field-flattener lens and CCD, would only be mounted to the back of the fold mirror once all of the detector testing and optimisation had been completed. This afforded us the uniquely wonderful opportunity of placing an F/18 white light “star” on the slit and visually observing the resulting spectrum, floating in mid-air above the slot in the fold mirror!

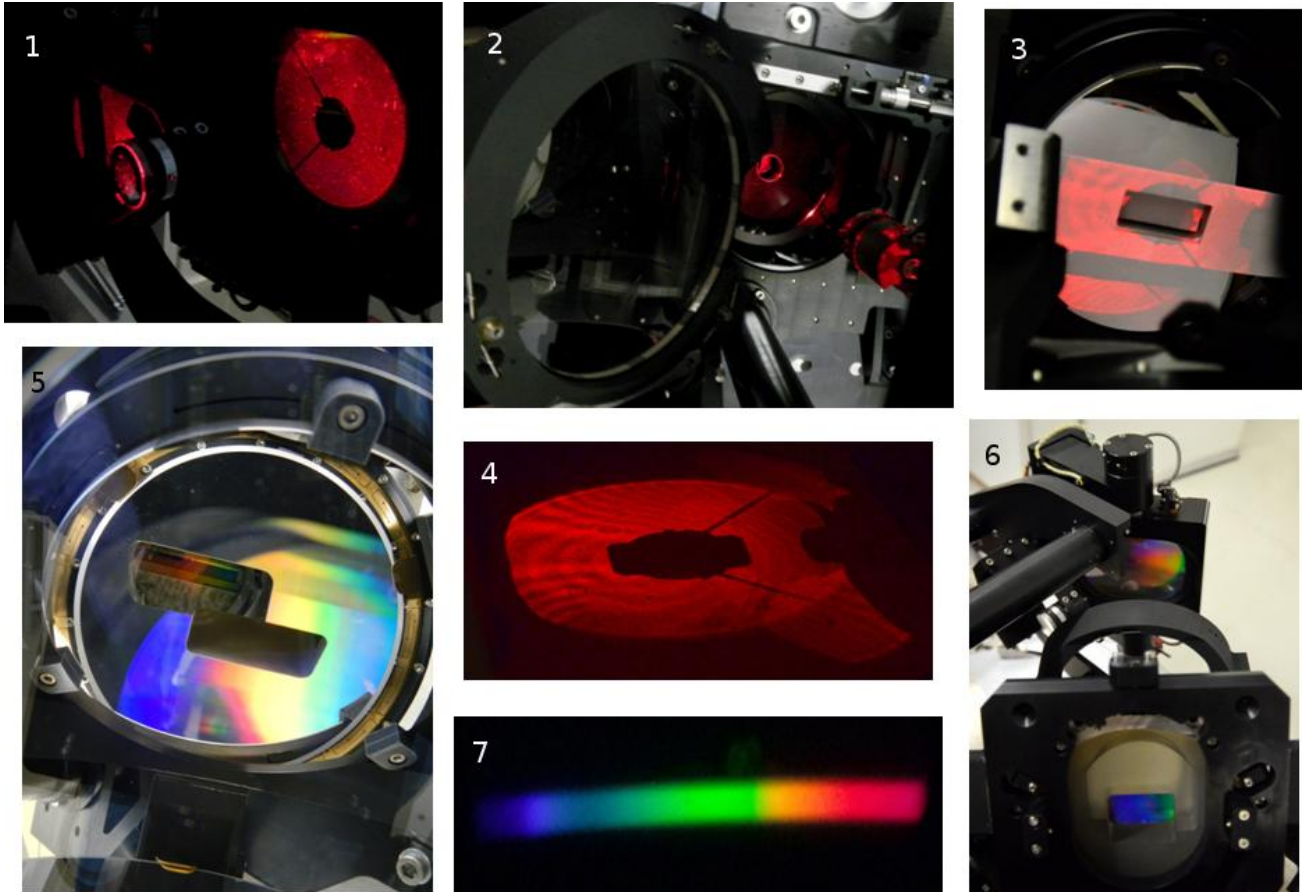


Figure 17. Various stages in the alignment of the SpUpNIC optics: 1 = collimator secondary (left) and grating (right) illuminated with the laser interferometer, 2 = collimator primary and rear of secondary similarly illuminated, 3 = positioning the central obscuration on the slot in the fold mirror, 4 = minimised obscuration seen on the primary mirror, 5 = the completed camera assembly, 6 = the focal plane is near to the slot in the fold mirror, 7 = photographic rendition of the visually observed spectrum.

The remaining optical challenges involved getting the CCD aligned with respect to the field-flattener lens, and optimally positioning the cryostat to complete the camera assembly. The CCD alignment was done using the AT, which was set up to be on the optical axis of the field-flattener lens. The CCD is clamped into a kinematic cradle unit that in turn bolts to the kinematic alignment jig, which locates in the lower section of the cryostat. The axial position of the CCD (just 4 mm behind the rear surface of the lens) was set using feeler gauges attached to the base of the CCD cradle using 100 micron thick Kapton tape. The CCD then served as a mirror, reflecting the AT spots produced by the two lens surfaces. The tip/tilt and decentre fine-adjusters on the alignment jig could then be used to tweak the cradle position until all of the return spots were centred on the AT crosshairs. Scotch-Weld 2216 epoxy was then injected into the various bonding holes to lock the CCD cradle to the G10 arms that bolt to the cryostat. The fine adjusters on the jig were also locked with epoxy to preserve their settings. After the epoxy had fully cured, the alignment jig could be removed and the rest of the cryostat assembled for subsequent testing.

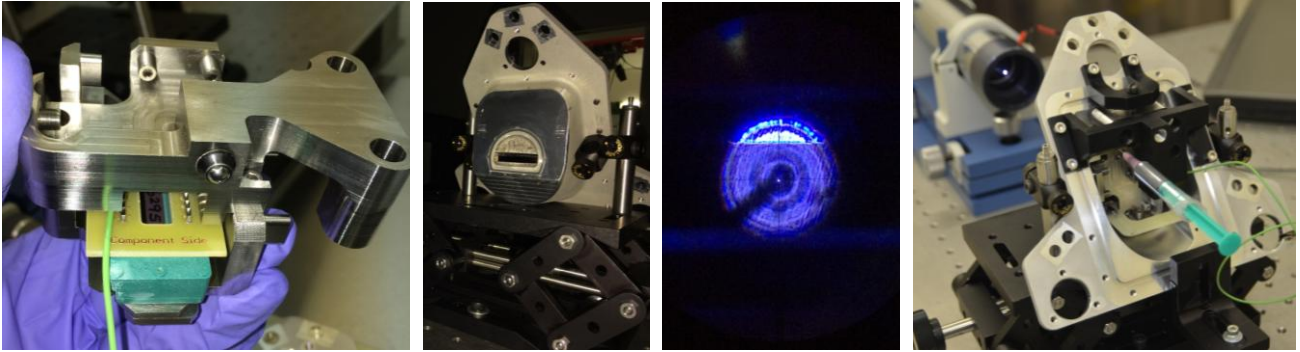


Figure 18. The CCD alignment jig attached to the cradle holding the chip (far left). The cryostat set up for the alignment of the CCD mounting assembly with respect to the field-flattener lens (left). One of the views through the AT during the CCD alignment process (right). Bonding the G10 arms (that bolt to the cryostat) to the aligned CCD cradle.

Upon completion of the remaining CCD tests, first with the electrical sample chip and then with the science CCD, the cryostat assembly (including the liquid nitrogen tank) could be fitted to the rest of the lower box components to complete the optical path. Adjustments to the cryostat alignment and camera focus were made using white light frames taken with the detector. Arc lines only became available once the new lower box structure was attached to the upper box that carries the arc lamps. The arcs were used to refine the focus, check the grating mechanism and test the different gratings.



Figure 19. The cryostat connected to the rest of the lower box (left), the lower box attached to the upper box (centre) and the largely complete assembly weighing in at approximately 400 kg (right).

Since the cryostat and/or the CCD may need to be removed periodically, both have kinematic mounting arrangements. The locked jig used to perform the CCD/window alignment is attached to the CCD whenever it has to be removed and re-installed. Similarly, the cryostat assembly was aligned to the rest of the camera optics and then the adjustable elements were locked with epoxy. Both these systems reliably relocate the relevant assemblies.

4. SPUPNIC PERFORMANCE

The upgraded spectrograph was installed on the telescope on 21 October 2015 and First Light was achieved early that evening. A five second snapshot of a bright ($V = 4.3$) A-type dwarf that we had used to check the telescope pointing and focus quickly confirmed that, at least to zeroth order, all was well with the new instrument.

The weather was largely uncooperative for most of that week and SpUpNIC was nervously handed over to an enthusiastic observer six nights later. The long-awaited spectrograph has been in demand ever since. Commissioning and trouble-shooting tasks have been attended to between observing runs and various software refinements have been applied. Formal qualification of the entire instrument will take place once final modifications are made to address the few remaining technical and operational issues. The most serious of which was mechanical instability of the grating mechanism, which severely compromises radial velocity programmes. We are cautiously optimistic that our latest intervention will have resolved this problem, but on-sky data is required to evaluate the behaviour of the system.

4.1 SpUpNIC vs Cassie Comparison

The throughput increase due to the spectrograph upgrade is demonstrated with low resolution (Grating 7) data that spans most of the spectral range of the instrument (see Fig. 20). A spectrophotometric standard star (LTT 377) was observed under photometric conditions with Cassie and later with SpUpNIC. The latter has roughly twice the sensitivity in the green (~5500 Å) and the ratio increases to about four further towards the blue (~4200 Å). However, the improvement in the red is somewhat disappointing due to the new CCD having lower quantum efficiency in the red than the old one did.

The combination of the new optics and the larger CCD has reduced the dispersion of the spectrograph, but also increased the wavelength range. Approximate values for the different gratings are given in Table 1. Comparisons between old and new data thus need to account for the larger pixels (if per pixel value are being considered), or the relative gains of the new and old systems (1.145 and 1.0, respectively) if the counts themselves are being compared. The effect of the dispersion change has been factored into the plots in Fig. 20.

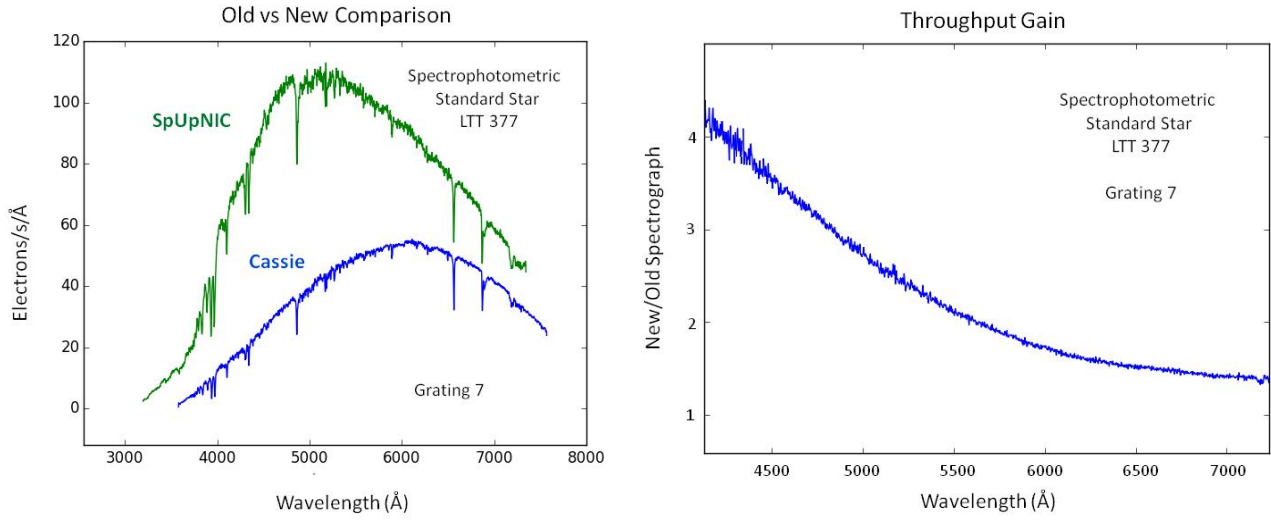


Figure 20. A spectrophotometric standard star was observed in photometric conditions with G7 using the old spectrograph (Cassie) and SpUpNIC. The better blue sensitivity of the new CCD makes a significant contribution towards the shorter wavelengths.

4.2 SpUpNIC Gratings

Table 1. Preliminary grating parameters (this table will be updated after final modifications are made to the grating assembly).

Grating	Lines per mm	Blaze Wavelength (Å)	Wavelength Range (Å)	Dispersion (Å/pixel)	Resolving Power	Star Filter	Arc Filter
G4	1200	4600	1250	0.625	2500	None	None
G5	1200	6800	1100	0.525	6500	GG495	GG495
G6	600	4600	2800	1.36	1000	None	None
G7	300	4600	5600	2.72	700	BG38	None
G8	400	7800	4100	2.21	1200	GG495	GG495
G9	830	7800	1700	0.835	2500	GG495	GG495
G10	1200	10000	950	0.470	5400	GG495	GG495
G11	600	10000	2600	1.25	1200	GG495	GG495
G12	300	10000	5600	2.75	1000	GG495	GG495

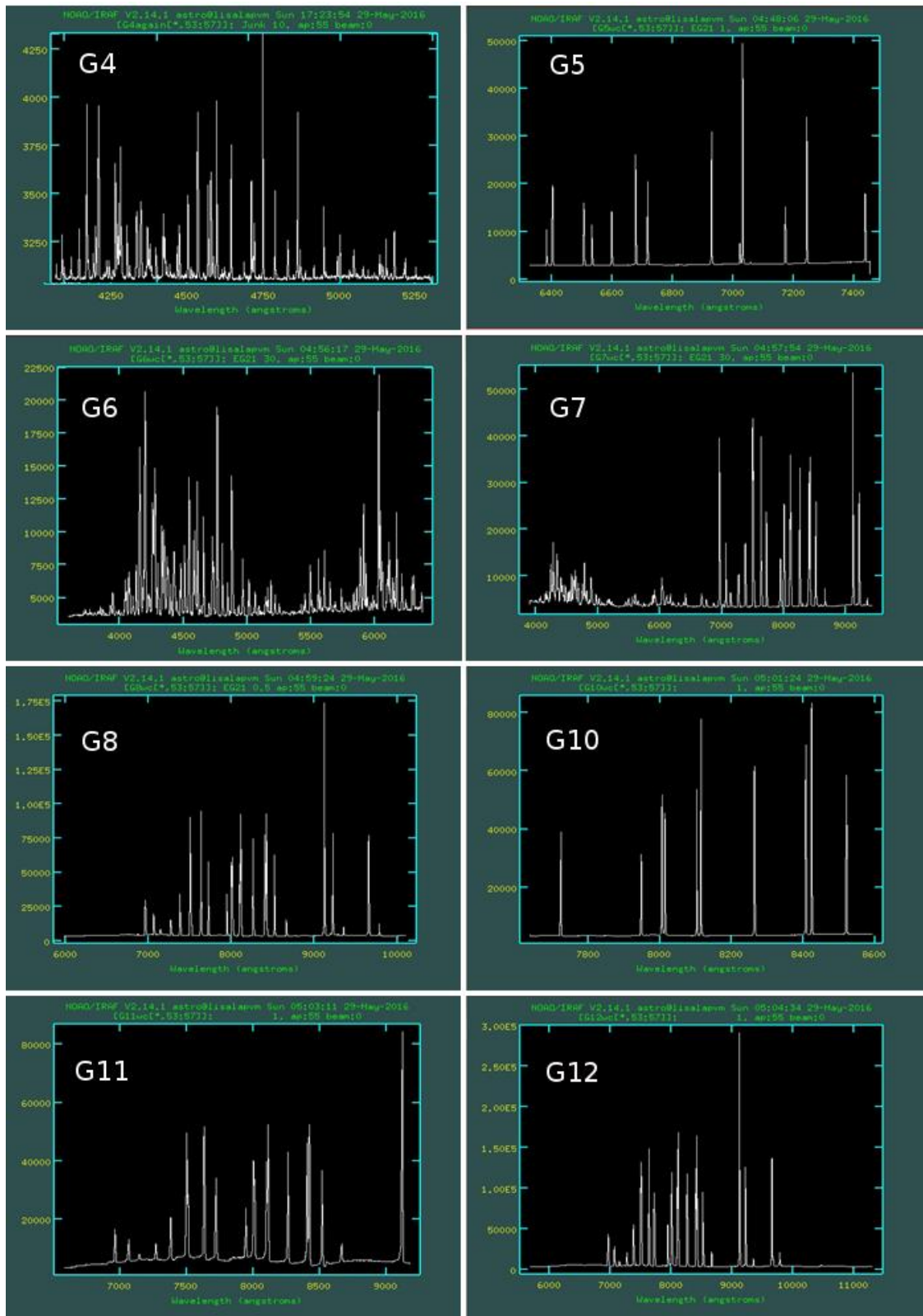


Figure 21. Representative wavelength calibrated arc spectra obtained with the various gratings. G9 is missing as the grating angle used did not yield useful lines, but it is intermediate between G10 and G11 in terms of its dispersion.

various gratings will follow now that the grating mechanism is fully reliable, and all of the documentation for the instrument will be completed.

5. SUMMARY

The Cassegrain Spectrograph Upgrade project has effectively yielded an entirely new low resolution optical spectrograph, the first to have been designed and built at the SAAO. This represents a step-increase in complexity over previous SAAO instrument development efforts: from the optical and mechanical design work involved, through the transition to the SDSU III CCD controller for the new detector package, software development in line with the SAAO's new instrumentation software framework, the implementation of a PLC system for controlling all of the mechanisms within the instrument, the in-house manufacturing of all the new hardware, through the assembly, integration, optical alignment, lab testing, installation, commissioning, documentation and ongoing support of the spectrograph. This formative experience has forged the Instrumentation team and will hugely benefit future instrument development initiatives at the SAAO. Many of the critical steps in the process have been described in photo-rich detail (and in some cases captured on video) on the SpUpNIC blog: <http://saaospup.blogspot.co.za/>.

This upgrade has substantially increased the throughput of the SAAO's workhorse instrument and the many improvements to the overall observing efficiency further streamline the acquisition and reduction of spectroscopic data. These advances are boosting the scientific productivity of the SAAO's 74-inch telescope – the second largest optical telescope on the African continent.

ACKNOWLEDGEMENTS

We sincerely thank John Booth for countless helpful discussions, great ideas and practical suggestions, as well as his unwavering support and endless good humour throughout the most challenging aspects of this marathon project.

It is with profound sadness that we dedicate this instrument to the memory of our beloved and most exceptional colleague, mentor and friend – Darragh O'Donoghue. Darragh started all of this in the late 1990s, when he took up the challenge of replacing the camera optics for the Cassegrain Spectrograph. His tireless efforts at SALT subsequently drew him away, but he was at the telescope for Cassie's last night on sky (6 October 2014). The brilliant, colourful and ethereally beautiful streak of light that SpUpNIC creates will forever remind us of the truly remarkable human being that we were so fortunate to know.

REFERENCES

- [1] Glass, I. S., "The Story of the Radcliffe Telescope", Quarterly Journal of the Royal Astronomical Society, 30: 33-58 (1989).
- [2] <http://saaospup.blogspot.com>
- [3] Stobie, R., Meiring, J. G., Buckley, D. A. H., "Design of the Southern African Large Telescope (SALT)", Proc. SPIE 4003, 355 (2000).
- [4] O'Donoghue, D., "Correction of spherical aberration in the Southern African Large Telescope (SALT)", Proc. SPIE 4003, 363 (2000).
- [5] Swat, A., O'Donoghue, D., Swiegers, J., Nel, L. and Buckley, D. A. H., "The optical design of the Southern African Large Telescope", Proc. SPIE 4837, 564 (2003).
- [6] Meiring, J. G., Buckley, D. A. H., "Southern African Large Telescope (SALT) project, progress and status after 4 years", Proc. SPIE 5489, 592 (2004).
- [7] O'Donoghue, D. E., Bauermeister, E., Carter, D. B., Evans, G. P., Koorts, W. P., O'Connor, J. E., Osman, F., van der Merwe, S., Bigelow, B., "SALTICAM: \$0.5M acquisition camera: every big telescope should have one", Proc. SPIE 4841, 465 (2003).
- [8] O'Donoghue, D. E. et al., "The image quality of the Southern African Large Telescope (SALT)", Proc. SPIE 7018, 32 (2008).
- [9] <http://saltiqmission.blogspot.com>

- [10] O'Donoghue, D. E., Crause, L. A., O'Connor, J. E., Strümpfer, F., Strydom, O. J., Sass, C., Brink, J. D., du Plessis, C., Wiid, E. P., Love, J., "Resolving the Southern African Large Telescope's image quality problems", *Opt. Eng.* 52 (8), 2013.
- [11] Crause, L. A. et al., "Performance of the Southern African Large Telescope (SALT) High Resolution Spectrograph (HRS)", *Proc. SPIE* 9147, 91476T (2014).
- [12] Crause, L. A., O'Donoghue, D. E., O'Connor, J. E., Strümpfer, F., "Use of a Faro Arm for optical alignment", *Proc. SPIE* 7739, 90 (2010).
- [13] Macfarlane, S. A. et al., "The OmegaWhite Survey for Short-Period Variables III : Follow-up Photometric and Spectroscopic Observations", submitted *MNRAS* (2016).